Proceedings of the ASME 2023
International Design Engineering Technical Conferences
and Computers and Information in Engineering Conference
IDETC/CIE2023
August 20-23, 2023, Boston Park Plaza, Boston

IDETC2023-116839

FATIGUE PREDICTION FOR REPETITIVE LIFTING

Shuvrodeb Barman

Mechanical and Aerospace Engineering Oklahoma State University Stillwater, Oklahoma 74078, USA

Ritwik Rakshit

Mechanical Engineering Texas Tech University Lubbock, Texas 79409, USA

Yujiang Xiang¹

Mechanical and Aerospace Engineering Oklahoma State University Stillwater, Oklahoma 74078, USA

James Yang

Mechanical Engineering Texas Tech University Lubbock, Texas 79409, USA

ABSTRACT

In this study, the fatigue progression and optimal motion trajectory during repetitive lifting task is predicted by using a 10 degrees of freedom (DOFs) two-dimensional (2D) digital human model and a three-compartment controller (3CC) fatigue model. The numerical analysis is further validated by conducting an experiment under similar conditions. The human is modeled using Denavit-Hartenberg (DH) representation. The task is mathematically formulated as a nonlinear optimization problem where the dynamic effort of the joints is minimized subjected to physical and task specific constraints. A sequential quadratic programming method is used for the optimization process. The design variables include control points of (1) quartic B-splines of the joint angle profiles; and (2) the three compartment sizes profiles for the six physical joints of interest - spine, shoulder, elbow, hip, knee, and ankle. Both numerical and experimental liftings are performed with a 15.2 kg box as external load. The simulation reports the human joint torque profiles and the progression of joint fatigue. The joint torque profiles show periodic trends. A maximum of 17 cycles are predicted before the repetitive lifting task fails, which also reasonably agrees with that of the experimental results (16 cycles). This formulation is also a generalized one, hence it can be used for other repetitive motion studies as well.

Keywords: Repetitive lifting, motion planning, fatigue model, and inverse dynamics optimization.

1. INTRODUCTION

Joint fatigue during a repetitive lifting task can greatly reduce the available muscle force capacity. Since fatigue is the cumulative result of various physiological and neurological processes occurring simultaneously, it is very hard to single out the contribution of any one phenomenon. This makes any fatigue-related force loss computation quite challenging [2, 5]. Software that can predict subject specific lifting strategies while taking the different weights associated with each lifting into consideration are paramount to prevent work related injury over time.

For the past few decades, researchers have developed various prediction models for lifting motion simulation based on kinematics and physics [4]. Also, optimization-based motion prediction algorithm development has made a significant progress during this time [12, 14-21]. These studies use gradientbased sequential quadratic programming (SQP) to solve the constrained nonlinear motion prediction optimization problems. Since gradient-based iterative optimization methods are still the most efficient methods for solving nonlinear problems, those predictions can be fairly accurate when the effect of fatigue during the task is not considered. However, the major limitation of these methods is the inability to correctly predict the fatigue progression during any repetitive task. To increase the accuracy of these predictions, the contribution of fatigue must be contemplated. Yet, apart from a couple of studies [1, 10], adding the contribution of fatigue in posture or motion prediction studies have seen little light. Any major work is yet to be published that incorporates the fatigue due to repetitive lifting.

¹ Corresponding author: yujiang.xiang@okstate.edu

To successfully study the contribution of fatigue, a rigorous mathematical modelling of the fatigue progression in human joints needs to be done. Fatigue models are mostly based upon analytical or experimental methods; hence it is quite complicated to incorporate those into numerical studies. Hence, apart from the preliminary work by Pereira that includes the fatigue study during elbow joint motion, little further study [7, 9] involving a complex model such as the full-body motion has been conducted. In our previous study [1], we have proposed a novel method to study the fatigue progression during a box-carrying posture task, but no motion is predicted.

This work aims to bridge that gap and extends our previous collaborative fatigue prediction study from a box-carrying task to a repetitive lifting motion prediction. The study aims to predict and validate the fatigue progression during this task. To predict the fatigue progression and optimal lifting strategy, an inverse dynamics optimization formulation is proposed. The lifting task is set up as a nonlinear programming (NLP) optimization problem. Dynamic effort is used as the objective function during the task, which is minimized using the SQP algorithm [8]. The optimization and experimental results are presented, and a valid comparison is established.

2. **METHOD**

In this section, the human model design, fatigue model integration and the experimental setup is discussed.

2.1 Human model

This study considers a 10-DOF 2D digital human model. The first three DOFs are global DOFs and refer to the movement of the whole body at hip joint in the global reference frame as indicated by the zero subscript in Figure 1. The DH approach is used to construct the model [1]. Furthermore, the positive direction of each physical joint rotation is also marked. The equations of motion (EOM) of the digital human are set up using the recursive Lagrangian dynamics formulation [1]. The system's dynamics equation can be written as:

$$\tau_{i} = tr\left(\frac{\partial \mathbf{A}_{i}}{\partial q_{i}}\mathbf{D}_{i}\right) - \mathbf{g}^{\mathrm{T}}\frac{\partial \mathbf{A}_{i}}{\partial q_{i}}\mathbf{E}_{i} - \mathbf{f}_{k}^{\mathrm{T}}\frac{\partial \mathbf{A}_{i}}{\partial q_{i}}\mathbf{F}_{i} - \mathbf{G}_{i}^{\mathrm{T}}\mathbf{A}_{i-1}\mathbf{z}_{0}$$
(1)

where the first term is inertia and Coriolis torque, the second term is the torque due to gravity, the third term is the torque due to external forces, and the fourth term is the torque due to external moments in equation (1). Here, $\mathbf{f}_k = [f_{kx} \quad f_{ky} \quad f_{kz} \quad 0]^{\mathrm{T}}$ is the external force applied on link k. For a detailed derivation of the EOM please refer to [14, 15].

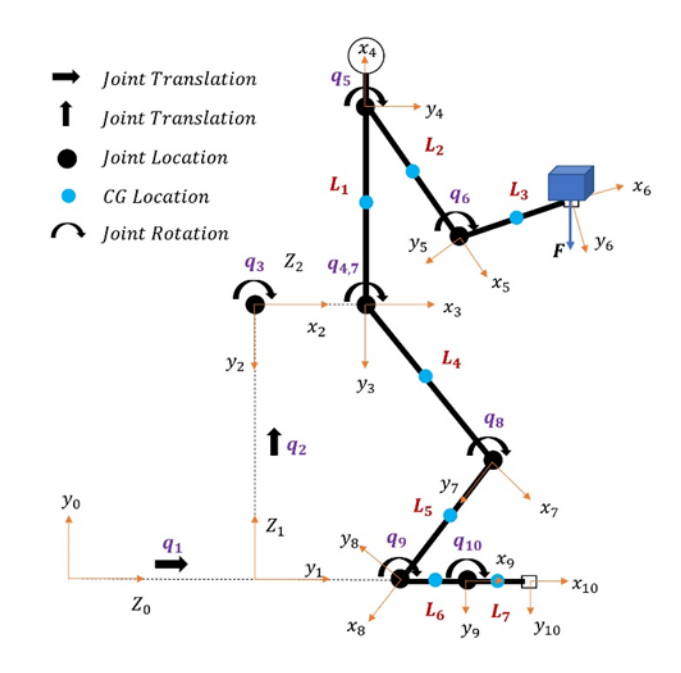


FIGURE 1: THE 2D HUMAN MODEL

2.2 Fatigue model

The three-compartment controller (3CC) fatigue model consisting of resting, active and fatigued compartments [11, 13] is used to study the repetitive fatigue progression. Figure 2 shows the schematic of this system and the flow between the compartments which is governed mathematically by the first order differential equations given by (2-4).

$$\frac{\mathrm{d}M_{Ri}(t)}{\mathrm{d}t} = -C_i(t) + R_i \times M_{Fi}(t) \tag{2}$$

$$\frac{\mathrm{d}M_{Ai}(t)}{\mathrm{d}t} = C_i(t) - F_i \times M_{Ai}(t) \tag{3}$$

$$\frac{dM_{Ri}(t)}{dt} = -C_i(t) + R_i \times M_{Fi}(t)$$

$$\frac{dM_{Ai}(t)}{dt} = C_i(t) - F_i \times M_{Ai}(t)$$

$$\frac{dM_{Fi}(t)}{dt} = F_i \times M_{Ai}(t) - R_i \times M_{Fi}(t)$$
(4)

where $M_{Ri}(t)$, $M_{Ai}(t)$ and $M_{Fi}(t)$ represents the resting, active and fatigued compartment sizes at time instant t. The fatigue (F_i) and recovery (R_i) coefficients for the joints of interest can be found in [13]. $C_i(t)$ is a bidirectional, time-varying torque activation-deactivation drive for the i^{th} joint at time instant twhich relates $M_{Ai}(t)$ and $M_{Ri}(t)$. The values of $C_i(t)$ satisfy the conditions given by equations (5-7).

If
$$M_{Ai}(t) < TL_i(t)$$
 and $M_{Ri}(t) > TL_i(t) - M_{Ai}(t)$,
 $C_i(t) = L_{Di} \times [TL_i(t) - M_{Ai}(t)]$ (5)

If
$$M_{Ai}(t) < TL_i(t)$$
 and $M_{Ri}(t) < TL_i(t) - M_{Ai}(t)$,
 $C_i(t) = L_{Di} \times M_{Ri}(t)$ (6)

$$If M_{Ai}(t) \ge TL_i(t),$$

$$C_i(t) = L_{Ri} \times [TL_i(t) - M_{Ai}(t)]$$
(7)

where L_{Di} denotes the force development factor and L_{Ri} denotes the relaxation factor. $TL_i(t)$ represents the target load for each joint at time instant t which is calculated using equation (8).

$$TL_{i}(t) = \begin{cases} \frac{\tau_{i}(t)}{\tau_{l}^{U}}, & for + ve \ torque \ direction \\ \frac{\tau_{i}(t)}{\tau_{l}^{L}}, & for - ve \ torque \ direction \end{cases} \tag{8}$$

where τ_i^U and τ_i^L denotes the maximum allowable torque for the i^{th} physical joint of interest during joint extension or flexion.

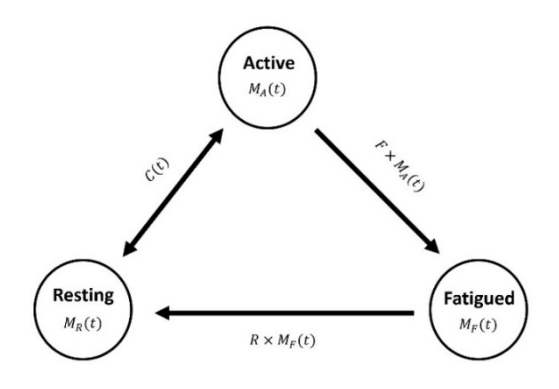


FIGURE 2: THREE-COMPARTMENT FATIGUE MODEL [13]

2.3 Repetitive lifting experiment

The sole participant of this pilot study is a 33-year-old healthy adult male, with a height of 1.69 m and a weight of 67.3 kg. An Xsens Awinda inertial motion capture system (Movella Inc., Henderson, Nevada, USA) running at 60 Hz is used to record the participant's motion data, while two Bertec force plates (Bertec Inc., Columbus, Ohio, USA) capture ground reaction forces and moments at 1000 Hz.

To determine the participant's maximum load carrying capacity, an empty box externally measuring $0.33~\text{m}\times0.33~\text{m}\times0.27~\text{m}$ is loaded with increasing weights. After each addition the subject is asked to determine whether they are comfortable lifting it from the ground to pelvis height and then replacing it once. The maximum combined lifting capacity determined this way is 15.2~kg.

For the data collection, the subject is asked to stand symmetrically with their toes just behind the leading edge of the force plates. The box is placed centrally at a distance the subject self-determined to be comfortable for lifting from. They are then instructed to lift the box up to pelvis height and lower it to its initial position without releasing it, and then repeat the process till exhaustion. An experimenter provides continuous guidance to help the subject achieve *near* consistent lift heights.

The synchronized collected data is processed in Visual3D (C-Motion Inc., Boyds, Maryland, USA) to calculate the joint angle profiles.

3. OPTIMIZATION FORMULATION

In this section, the elements of the constrained optimization formulation are discussed for a single cycle of the repetitive box lifting task. Note that, each lifting cycle is considered as a two-phased motion study, where the first half of the total time is spent on lifting the box up to a specified location (0.000, 1.088, 0.417), meter, and the remaining half time is used to bring the box back down to its original location (0.000, 0.070, 0.418), meter.

3.1 Design variables

Since the motion optimization is carried out in joint space, the joint angle profiles are considered as a part of the design variables set. From the three-compartment controller (3CC) fatigue model, the resting compartment size profiles, the active compartment size profiles, and the fatigued compartment size profiles are also considered as the design variables to study the fatigue progression during the repetitive lifting task. A recursive quartic B-spline interpolation is used to transform these time-dependent parameters from a continuous-time domain to a discrete-time domain. This way, the spline control points can become the design variables, which makes imposing constraints easier. The complete design variables set can then be expressed by equation (9).

$$\mathbf{x} = \begin{bmatrix} \mathbf{P}_{q_i}^T & \mathbf{P}_{M_{Bi}}^T & \mathbf{P}_{M_{Ai}}^T & \mathbf{P}_{M_{Fi}}^T \end{bmatrix}^T \tag{9}$$

The initial guess for all the joint angles, active, resting and fatigue compartment sizes are set to zero, but the resting compartment sizes are set to 1. The duration for each cycle is set as 3.0 seconds. The optimization problem is solved using SNOPT software which uses a sequential quadratic programming (SQP) algorithm.

3.2 Objective function

The goal of this study is to minimize the dynamic effort of all the physical joints, mathematically given by the expression shown in equation (10).

minimize
$$\int_0^T \sum_{i=4}^{10} \left[w_\tau \left(\frac{\tau_i}{\tau_i^U - \tau_i^L} \right)^2 + w_a \left(\frac{a_i}{a_{max}} \right)^2 \right] dt \qquad (10)$$

where T denotes the total duration of each lifting cycle, i denotes the physical joints considered for the motion study, τ_i denotes the i^{th} joint torque, τ_i^U and τ_i^L are upper and lower limits of the joint torques, w_{τ_i} denote the weights associated with the i^{th} joint torque, α_i denote the local angular accelerations of the physical joints and w_{α_i} denote the weights associated with local angular accelerations. The weights were all set to 1.

3.3 Constraints

Both time-dependent and time-independent constraints are considered for the optimization formulation of each cycle of the

repetitive task. For the entire time interval, 10 time-dependent constraints are considered. They are:

- (1) joint angle limits,
- (2) joint torque limits,
- (3) foot contacting position,
- (4) zero-moment point (ZMP) location,
- (5) box forward position,
- (6) collision avoidance,
- (7) monotonically changing wrist velocity,
- (8) the differential equations for resting, active and fatigued compartment sizes,
- (9) unit summation condition and
- (10) residual capacity condition.

In addition to these 10 constraints, 3 more time-independent constraints are also applied. They are:

- (11) initial and final box locations,
- (12) static conditions at the beginning, mid-time, and the end of the motion, and
- (13) the initial, quarter-time, half-time, three-quarters-time, and the final joint angles of the six physical joints of interest.

Note that the time-dependent constraints are calculated sequentially in the optimization process at every time discretization point. In contrast, optimization calculates the time-independent constraints at a specific time.

The optimization formulation for a single cycle of the repetitive task discussed in subsections 3.1-3.3 is repeated until SNOPT fails to find an optimal solution for the current cycle. The fatigue compartment size is set to zero at the start of only the first cycle of the optimization process. While simulating the process for the repetitive task, starting with the second cycle, the time-independent compartment size continuity constraints given in equations (11-13) are imposed.

$$M_{Ri\ k}(0) = M_{Ri\ (k-1)}(T) \tag{11}$$

$$M_{Ai_{-k}}(0) = M_{Ai_{-(k-1)}}(T) \tag{12}$$

$$M_{Fi\ k}(0) = M_{Fi\ (k-1)}(T) \tag{13}$$

Also, to ensure a general increase in fatigue compartment size across all six physical joints of interest, the derivatives of the final compartment sizes from the optimal result of the previous cycle are also set equal to the derivatives of the initial compartment sizes of the current cycle.

$$\dot{M}_{Ri\ k}(0) = \dot{M}_{Ri\ (k-1)}(T) \tag{14}$$

$$\dot{M}_{Ai_{-}k}(0) = \dot{M}_{Ai_{-}(k-1)}(T) \tag{15}$$

$$\dot{M}_{Fi\ k}(0) = \dot{M}_{Fi\ (k-1)}(T) \tag{16}$$

An additional constraint given by equation (17) ensures the continuity between joint angles from one cycle to the next.

$$q_{i,k}(0) = q_{i,(k-1)}(T)$$
(17)

The subscripts k and (k-1) denote the parameters in equations (11-17) at initial and final times of the k^{th} and $(k-1)^{th}$ cycle, respectively with k=2,3,4,...,niter.

4. RESULTS

The optimal motion and the fatigue progression is predicted using the optimization formulation described in section 3 for a 1.69 m tall subject who weighs about 67.3 kg while he repetitively lifts a 15.2 Kg box. A maximum of 17 cycles are predicted before the repetitive task fails. The simulation is run on a laptop with an 11th Gen Intel Core i9-11900H processor clocked at 2.50 GHz base speed, which features 8 cores, 16 logical processors and 32 GB RAM. The joint limits, foot contacting position, initial and final box locations, residual capacity, collision avoidance, compartment size continuity and unit summation constraints are active during the optimization process.

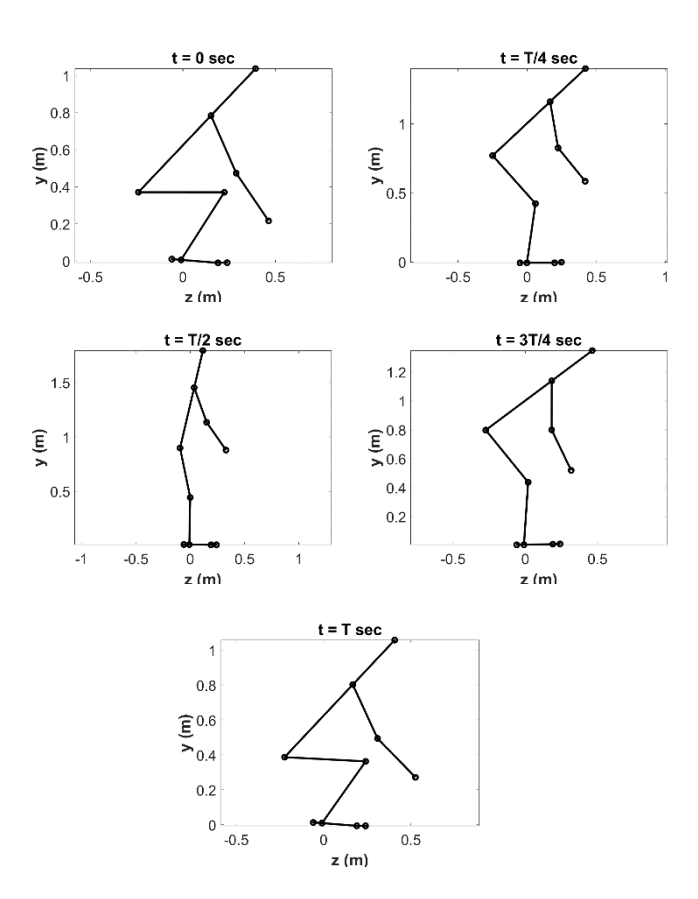
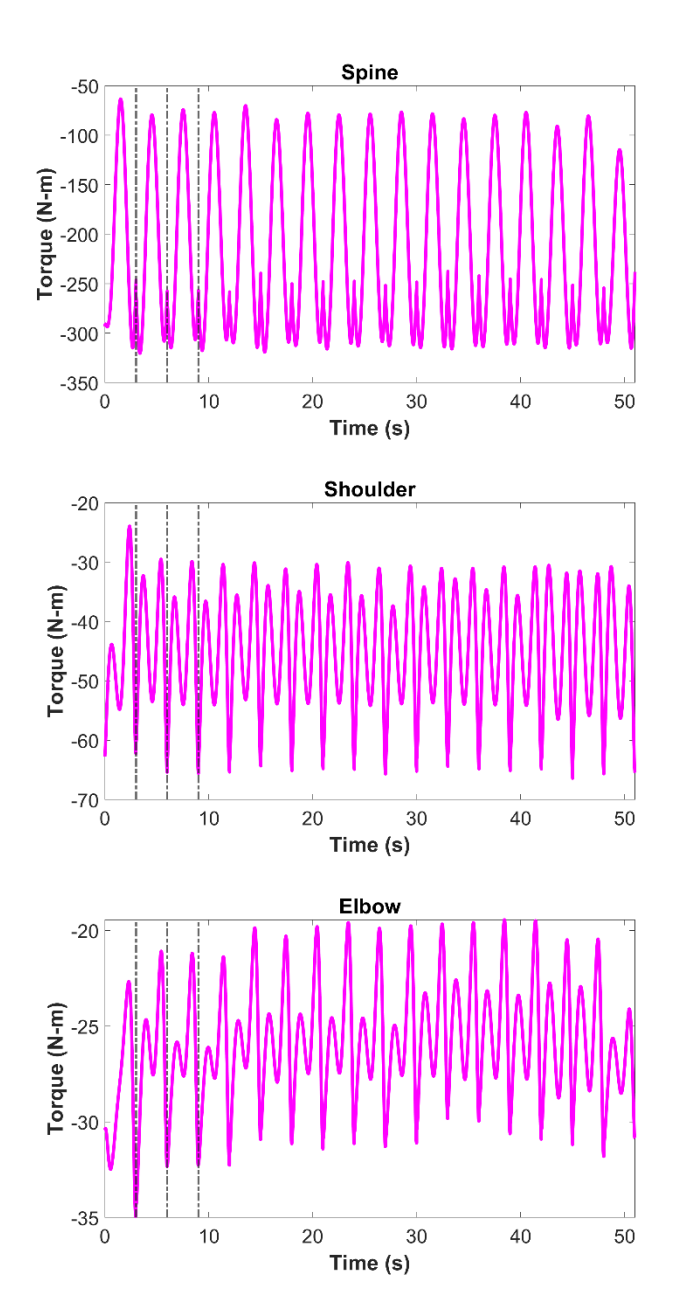


FIGURE 3: SIMULATION SNAPSHOTS

First, Figure 3 illustrates snapshots of the predicted 2D human lifting motion from the simulation at the initial, quarter-time, half-time, three-quarters-time, and the final time instant. Furthermore, the torque profiles for the same joint motions are shown in Figure 4. Finally, the fatigue progression status for the

six physical joints of interest is shown in Figure 5 which is characterized by the three compartment size profiles. In all these figures, the first three cycles are marked by the gray dashed lines.



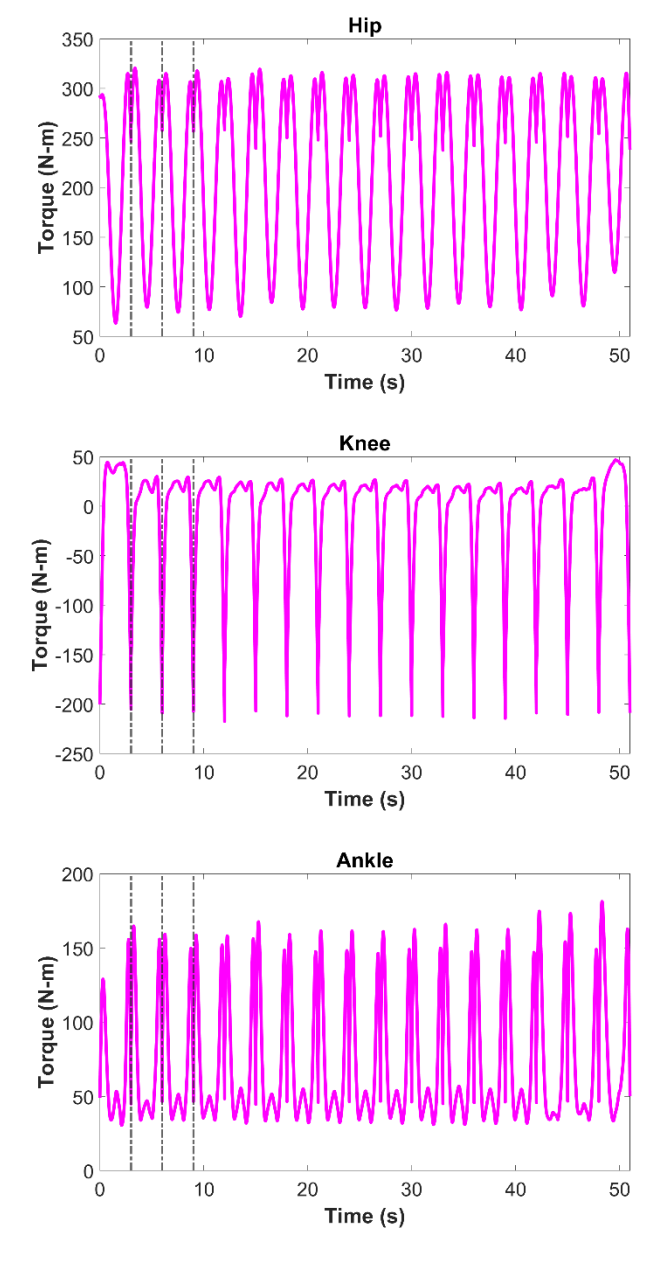
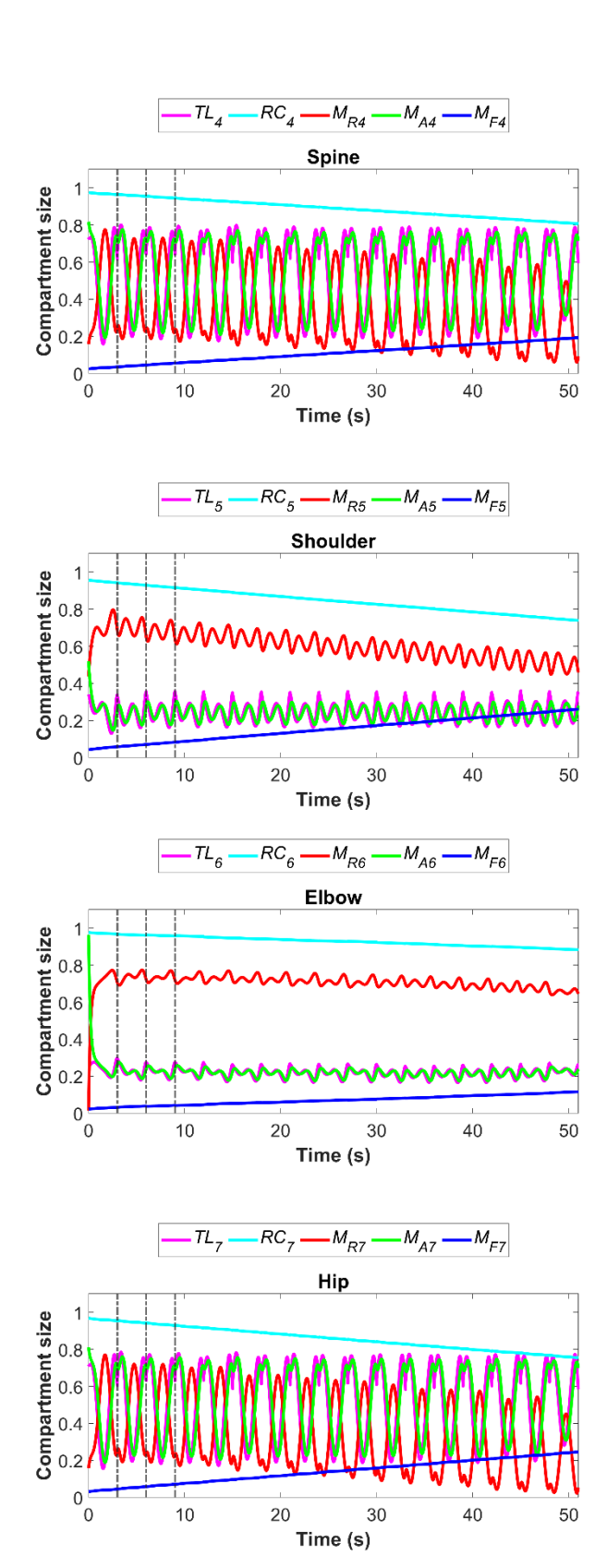


FIGURE 4: JOINT TORQUE PROFILES



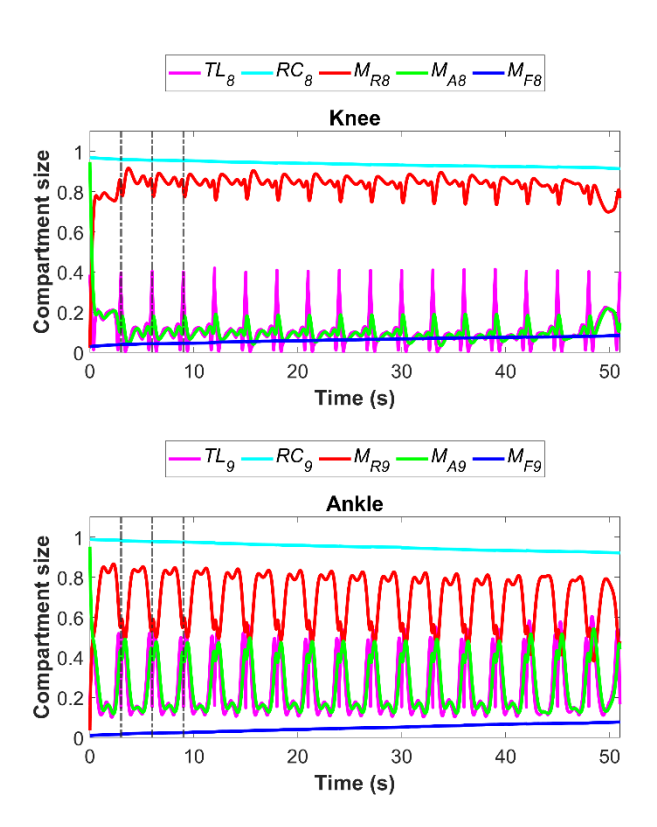


FIGURE 5: JOINT FATIGUE PROGRESSION

5. DISCUSSION

During the first half-duration of each cycle, the shoulder flexes, elbow flexes and the hip extends until the box is lifted to the desired location. During the second half-duration of each cycle, the opposite motion trend is followed by the joints. These trends are further confirmed by the motion trajectory shown in Figure 3. The joint torque profiles show the periodic trends as illustrated in Figure 4. During the motion of all six physical joints of interest, the active compartment size profiles tend to track the general shape of the target load profiles. The resting compartment size profiles follow the opposite direction of the active compartment size profiles for all the joints, satisfying the governing equations of the 3CC fatigue model where the resting compartment supports the active compartment as necessary throughout the duration of the entire repetitive task. This is also consistent with the unit summation constraints. As the fatigue compartment size profiles grow, less room is available to use from the resting and active compartment profiles. The task is considered to have failed when the residual capacity, $RC_i(t) =$ $M_{Ai}(t) + M_{Ri}(t)$ of one or more of the joints of interest falls below the target load (Hip joint for this study).

Though the number of predicted repetitions before the task fails is close to that of the experimental one (16 experimental cycles as opposed to numerically predicted 17 cycles), but they are not the same. Because, during the repetitive lifting task, the

lifting strategy of the human subject cannot be kept constant from cycle to cycle. This will contribute to the variations in cycle time, speed of the lifting motion, even the final location of the box. An average cycle time is used in the optimization formulation, which largely contributes to the variation in the predicted results.

6. CONCLUSION

In this study, the fatigue progression and the optimal motion trajectory during a repetitive lifting task are predicted using an inverse dynamics optimization formulation. SNOPT, a gradient-based optimizer, effectively solved the complex non-linear optimization problem. Simulation results are found to be reasonable. The simulation results are compared to the experimental data for the total number of cycles repeated before failure. Furthermore, the proposed optimization formulation can be used to predict fatigue status and optimal motion trajectory during any type of repetitive task during the manual material handling (MMH) process, thus enhancing the chance to reduce work related injury. Our next goal is to update the optimization formulation using genetic algorithm (GA) to obtain a global optimal solution in the future.

ACKNOWLEDGEMENTS

This study is supported by the National Science Foundation (CBET 2014281 and 2014278).

REFERENCES

- [1] Barman, S., Xiang, Y., Rakshit, R., & Yang, J., 2022, Joint fatigue-based optimal posture prediction for maximizing endurance time in box carrying task. *Multibody System Dynamics*, 55, 323-339.
- [2] Barry, B. K., & Enoka, R. M., 2007, The neurobiology of muscle fatigue: 15 years later. *Integrative and Comparative Biology*, 47 (4), 465-473.
- [3] Cheng, H., Obergefell, L., & Rizer, A., 1994, *Generator of body (GEBOD) manual*. AL/CF-TR-1994-0051, Armstrong Laboratory, Air Force Materiel Command, Wright-Patterson Air Force Base, Ohio.
- [4] Daynard, D., Yassi, A., Cooper, J., Tate, R., Norman, R., & Wells, R., 2001, Biomechanical analysis of peak and cumulative spinal loads during simulated patient-handling activities: A substudy of a randomized controlled trial to prevent lift and transfer injury of health care workers. *Applied Ergonomics*, 32 (3), 199-214.
- [5] Fitts, R. H., 1994, Cellular mechanisms of muscle fatigue. *Physiological Reviews*, 74 (1), 49-94.
- [6] Frey-Law, L. A., Looft, J. M., & Heitsman, J., 2012, A three-compartment muscle fatigue model accurately predicts joint-specific maximum endurance times for sustained isometric tasks. *Journal of Biomechanics*, 45 (10), 1803-1808.

- [7] Giat, Y., Mizrahi, J., & Levy, M., 1993, A musculotendon model of the fatigue profiles of paralyzed quadriceps muscle under FES. *IEEE Transactions on Biomedical Engineering*, 40 (7), 664-674.
- [8] Gill, P. E., Murray, W., & Saunders, M. A., 2005, SNOPT: An SQP algorithm for large-scale constrained optimization. Society for Industrial and Applied Mathematics, 47 (1), 99-131.
- Hawkins, D., & Hull, M. L. (1993). Muscle force as affected by fatigue: *Mathematical model and experimental verification*. *Journal of biomechanics*, 26 (9), 1117-28.
- [9] Ma, L., Chablat, D., Bennis, F., & Zhang, W., 2009, A new simple dynamic muscle fatigue model and its validation. *International Journal of Industrial Ergonomics*, 39 (1), 211-220.
- [10] Pereira, A. F., Silva, M. T., Martins, J. M., & de Carvalho, M., 2011, Implementation of an efficient muscle fatigue model in the framework of multibody systems dynamics for analysis of human movements. *Proceedings of the Institution of Mechanical Engineers, Part K: Journal of Multi-Body Dynamics*, 225 (4), 359-370.
- [11] Rakshit, R., Barman, S., Xiang, Y., & Yang, J., 2022, Sensitivity analysis of sex- and functional muscle group-specific parameters for a three-compartment-controller model of muscle fatigue. *Journal of Biomechanics*, 141, 111224.
- [12] Song, J., Qu, X., & Chen, C.-H., 2016, Simulation of lifting motions using a novel multi-objective optimization approach. *International Journal of Industrial Ergonomics*, 53(100), 37-47.
- [13] Xia, T., & Frey Law, L. A., 2008, A theoretical approach for modeling peripheral muscle fatigue and recovery. *Journal of Biomechanics*, 41 (14), 3046-3052.
- [14] Xiang, Y., Arora, J., & Abdel-Malek, K., 2009, Optimization-based motion prediction of mechanical systems: Sensitivity analysis. *Structural and Multidisciplinary Optimization*, 37, 595-608.
- [15] Xiang, Y., Arora, J., Rahmatalla, S., Marler, R., Bhatt, R., & Abdel-Malek, K., 2010, Human lifting simulation using a multi-objective optimization approach. *Multibody System Dynamics*, 23, 431-451.
- [16] Xiang, Y., Cruz, J., Zaman, R., and, Yang, J., 2021, Multi-objective optimization for two-dimensional maximum weight lifting prediction considering dynamic strength. *Engineering Optimization*, 53(2), 206-220.
- [17] Wang, Q., Xiang, Y., Kim, H.J., Arora, J.S., Abdel-Malek, K., 2005. Alternative formulations for optimization-based digital human motion prediction. *Proceedings of 2005 Digital Human Modeling for Design and Engineering Symposium*, June 14-16, Iowa City, IA. SAE Technical Paper 2005-01-2691.
- [18] Chung, H.J., Xiang, Y., Mathai, A., Rahmatalla, S., Kim, J., Marler, T., Beck, S., Yang, J., Arora, J., Abdel-Malek, K., Obusek, J., 2007, A robust formulation for prediction of human running. *Proceedings of 2007 Digital Human Modeling for Design and Engineering Symposium*, June 12-14, Seattle, WA. SAE Technical Paper 2007-01-2490.

- [19] Xiang, Y., 2019. An inverse dynamics optimization formulation with recursive B-spline derivatives and partition of unity contacts: Demonstration using two-dimensional musculoskeletal arm and gait. *ASME Journal of Biomechanical Engineering*, 141(3), 034503.
- [20] Xiang, Y., Arefeen, A., 2020, Two-dimensional team lifting prediction with floating-base box dynamics and grasping force coupling. *Multibody System Dynamics*, 50, 211-231.
- [21] Zaman, R., Arefeen, A., Quarnstrom, J., Barman, S., Yang, J., & Xiang, Y., 2022. Optimization-based biomechanical lifting models for manual material handling: A comprehensive review. *Proceedings of the Institution of Mechanical Engineers, Part H: Journal of Engineering in Medicine*, 236(9), 1273-1287.